Simultaneous design of proportional–integral–derivative controller and measurement filter by optimisation

Soltesz, Kristian; Grimholt, Chriss; Skogestad, Sigurd

Published in:
IET Control Theory and Applications

DOI:
10.1049/iet-cta.2016.0297

2016

Document Version:
Peer reviewed version (aka post-print)

Simultaneous Design of PID Controller and Measurement Filter by Optimization

Kristian Soltesz[1,*], Chriss Grimholt[2], Sigurd Skogestad[3]

[1]Department of Automatic Control, Lund University, Lund, Sweden
[2,3]Department of Chemical Engineering, Norwegian University of Science and Technology, Trondheim, Norway
[*]kristian@control.lth.se

Abstract: A method for optimization of PID controller parameters and measurement filter time constant is presented. The method differs from the traditional approach in that the controller and filter parameters are simultaneously optimized, as opposed to standard, sequential, design. Control performance is maximized through minimization of the integrated absolute error (IAE) caused by a unit step load disturbance. Robustness is achieved through $\mathcal{H}_\infty$ constraints on sensitivity and complementary sensitivity. At the same time, noise attenuation is enforced by limiting either the $\mathcal{H}_2$ or $\mathcal{H}_\infty$ norm of the transfer function from measurement noise to control signal. The use of exact gradients makes the synthesis method faster and more numerically robust than previously proposed alternatives.

1. Introduction

1.1. Motivation

The PID controller is by far the most widely used controller structure. Consequently, there exist an abundance of methods for PID synthesis. A majority of these aim at achieving sufficient load disturbance rejection (regulatory control) and robustness to plant model uncertainty. Most PID synthesis methods do not explicitly consider reference tracking (servo control). One reason for this might be that reference tracking can be achieved independently through a two degrees of freedom (2DOF) design scheme, such as [1]. Furthermore, regulatory control performance is more important than servo *ditto* in most (process) industrial applications, and controllers which achieve adequate regulatory control often also have acceptable reference tracking behavior.

There exist several performance measures to evaluate regulatory control performance. Two well-established such measures are the integrated error (IE) and integrated absolute error (IAE), defined through (7) and (6), respectively. In their context *error* refers to that resulting from a load disturbance unit step. The IAE has an advantage over the IE in that it punishes oscillatory load responses. The two performance measures are further discussed in Section 2.2.1.

When minimizing the IAE (but also the IE, or other measures of regulatory control performance) – even under robustness constraints – it is common to end up with controllers of very high gain from measurement (plant output) noise to control signal (plant input). These controllers can be practically useless, as will be demonstrated in Section 5, and shown in Figure 6. The typical approach to alleviate this problem, is to replace the derivative term of the PID control law, by a

low-pass filtered version [2]. This introduces at least one additional parameter – that of the filter. In many industrial controllers, the filter parameter is automatically set to a fixed ratio of the derivative time T_d of (4).

It was argued in [3], that filtering the entire measurement signal is preferential to only filtering the derivative term. This corresponds to connecting a low-pass filter in series with the PID controller, as shown in Figure 1. Furthermore, it was suggested to use (at least) a first-order filter for PI controllers, and a second-order filter for PID controllers, to achieve high-frequency roll-off.

Regardless of which of the above (or other) filter structures is used, the industrially established synthesis procedure is sequential. It comprises first choosing the gains of the PID controller, and subsequently tuning the filter to achieve acceptable noise rejection. Alternatively, the filter is initially fixed, whereupon the controller is synthesized. This approach works well when the resulting filter bandwidth lies significantly above that of the controller. However, if the noise spectrum is such that the bandwidths overlap, the filter will not only affect noise attenuation, but also robustness and control performance. This problem occurs regularly and suggests that the controller and filter should be simultaneously designed.

1.2. Previous Work

The problem of simultaneous design of controller and filter has been studied in a number of publications. A survey of relevant ones known to the authors is given below, to produce a reference frame for the work to be presented.

In [4], an approximate formula is used to compute a filter time constant, from the derivative gain and a noise sensitivity constraint. One step further towards truly simultaneous design is taken in [5], where an iteration between controller synthesis (by optimization) and filter design, is used. First, a controller which minimizes IE, subject to an $\mathcal{H}_\infty$ constraint on S, is obtained. Subsequently, a filter is designed for the series connection of the plant and the obtained controller. The filter is then assumed to be part of the plant model, and the procedure is iterated, until it converges. Similar, iteration-based, methods are presented in [6, 7]. For industrially relevant problems it seems (but has not been proven) that these iterative methods converge.

All methods mentioned so far, involve either solving a sequence of optimization problems [7] (which can be very time consuming), or using approximate formulae [6] (which does not guarantee optimality or constraints). The contributions [8, 9] propose a truly simultaneous design. An optimization problem with objective $\min \|PS/s\|_\infty$, and $\mathcal{H}_\infty$ constraints on S and Q is considered. Optimization is carried out over the parameters of a parallel form PID controller in series with a first-order low-pass filter. While the constraints are industrially well-established, the $\mathcal{H}_\infty$-objective is not. (However, it can be thought of as an approximation of IAE, as shown in [10].) In [11], Matlab-code is presented to perform the suggested optimization. The code is very compact and simple to read, but suffers numerical issues, as pointed out in Section 3.3.

In [12], a parallel form PID controller, given by any chosen design method, is converted into a PID controller with derivative filter. The filter is chosen in relation to the closed-loop cut-off frequency or high-frequency gain, such that the effect on nominal performance and robustness is limited. A similar approach is presented in [13], in order to produce tuning rules for the measurement-filter time constant. These rules are based solely on the controller parameters, and different rules apply, depending on which method was used for controller synthesis (SIMC [14] or AMIGO [15]). The method provides a free tuning parameter, affecting the trade-off between robustness and noise sensitivity.

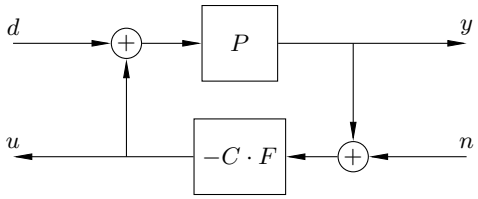

Fig. 1. *The considered control system structure.*

In [16], a particle swarm method is applied to a mixed-objective optimization problem, aiming at maximizing controller gain, while punishing the $\mathcal{H}_\infty$ norm of S and T, as well as the $\mathcal{H}_2$ norm of Q. A weighing of the different objective terms is proposed, but not motivated. In particular, this weighing may need to be changed depending on P and the spectral density of the noise signal.

Finally, [3, 17] propose the problem formulation adopted in this work, where IAE is minimized, under $\mathcal{H}_\infty$ constraints on S, T and an $\mathcal{H}_2$ constraint on Q. (We will also consider the $\mathcal{H}_\infty$ version of the last constraint.) This formulation is based on industrially established performance and robustness measures. However, the optimization used in [3, 17] relies on finite difference approximations of (objective and constraint) gradients. Apart from slow execution time, the use of finite differences easily leads to poor (or no) convergence, even in the simpler case of controller synthesis with a fixed filter [18].

To summarize, most of the mentioned methods [3, 7, 8, 11, 16, 17] propose simultaneous controller synthesis and filter design by optimization. However, they use the (simplex-like) Nelder-Mead method [19], gradient methods based on finite difference approximations [3, 8, 11, 17] or particle swarm methods [16] to find a solution. These methods all come with disadvantages: Gradient-free methods are known to be slow and care must be taken when gridding the parameter space. Using gradient methods, with finite difference approximations of the gradients, results in poor (or no) convergence within the considered context, as pointed out in [18]. Particle swarm methods require carefully chosen heuristics and provide little insight into the problem to be solved.

1.3. Novelty

This paper introduces an optimization-based tuning method for simultaneous PID controller and measurement filter synthesis. As opposed to most previous work, the measurement filter and controller are simultaneously designed by constrained optimization. The main novelty lies in the use of exact (analytic) gradients, to facilitate numerical robustness. Furthermore, the method eliminates the need for manual *a priori* selection of PID subtype (P, PI, PID, I, ID, PD, D). This selection is instead implicitly handled by the optimization.

2. Problem Formulation

2.1. Definitions

A synthesis scenario for the control system shown in Figure 1 will be considered. It consists of a linear time invariant single-input-single-output plant P, controller C, and measurement filter F. The objective is to achieve plant output $y = 0$ by means of the control signal u, in the presence of load disturbances d and measurement noise n. The standard deviations of n is denoted σ_n, and the resulting standard deviation of u is σ_u.

The single-input, single-output (SISO) controller C, the filter F and their combined parameter vector θ are defined

$$C(s) = \left(k_p + \frac{k_i}{s} + k_d s \right), \tag{1}$$

$$F(s) = \frac{1}{T_f^2 s^2 + T_f \sqrt{2} s + 1}, \tag{2}$$

$$\theta = \begin{bmatrix} k_p & k_i & k_d & T_f \end{bmatrix}^T \in \mathbb{R}_+^4. \tag{3}$$

The parametrization (1) is chosen in favor of the classic one

$$C(s) = K \left(1 + \frac{1}{T_i s} + T_d s \right), \tag{4}$$

as the former is linear in its parameters. (It is also more general, as for instance $\begin{bmatrix} k_p & k_i & k_d \end{bmatrix} = \begin{bmatrix} 0 & 1 & 1 \end{bmatrix}$ lacks an equivalent controller on the form (4).)

This paper focuses on using analytic expressions of gradients to optimize the controller parameters. The gradient operator, with respect to θ, will be denoted ∇. From here on, arguments of transfer functions and signals will be dropped, whenever the transform domain is clearly given by the context. The loop-transfer function is denoted $G = PCF$. Sensitivity and complementary sensitivity are defined $S = 1/(1+G)$, and $T = 1 - S = G/(1+G)$, respectively. Furthermore, the noise sensitivity, being the transfer function from measurement noise n to control signal u, is $Q = -CFS$.

The error caused by a unit load step disturbance d (see Figure 1) is

$$e(t) = -\mathcal{L}^{-1} \left(S(s) P(s) \frac{1}{s} \right). \tag{5}$$

The *load step* integrated absolute error (IAE) is then defined as

$$\text{IAE} = \int_0^\infty |e(\tau)| d\tau. \tag{6}$$

In addition we will consider the mathematically more convenient integrated error (IE)

$$\text{IE} = \int_0^\infty e(\tau) d\tau. \tag{7}$$

2.2. Optimization Problem

The considered optimization problem is

$$\begin{aligned} \underset{\theta}{\text{minimize}} \quad & \text{IAE}, \\ \text{subject to} \quad & \|S\|_\infty \leq M_s, \\ & \|T\|_\infty \leq M_t, \\ & \frac{\sigma_u}{\sigma_n} \leq M_q, \end{aligned} \tag{8}$$

where M_s, M_t and M_q are scalar constraint levels. It was recommended in [2] to keep M_s and M_t within the range $1.4 - 1.8$. The third constraint, enforcing noise attenuation by constraining the ratio between control signal and noise standard deviations, is the topic of Section 4.

2.2.1. Performance: The idea of posing PID design as a constrained optimization problem stretches back at least three decades. In early work [5, 20] the performance objective was to minimize the IE, as defined in Section 2.1. It was shown in [5] that minimization of the IE is equivalent to maximization of the integral gain k_i of (1). This constitutes a convex objective in the parameter vector θ (3), motivating the popularity of the IE as (inverse) performance measure.

If the load step response e (5) lacks zero crossings, it is evident from (7) and (6) that IE = IAE. Furthermore, well-damped control systems yield IE $\approx$ IAE. However, oscillatory systems, with consecutive zero crossings of e, may result in IE $\ll$ IAE. It is therefore preferential to minimize the IAE, in favor of the IE, in order to avoid oscillatory behavior. While minimization of the IAE does not constitute a convex objective, it can be efficiently performed using gradient methods [18], as further explained in Section 3.3.

2.2.2. Robustness: It is customary, and industrially well-established, to enforce robustness of the control system through $\mathcal{H}_\infty$ constraints on S and T. These constraints limit the magnitude of S and T, and it is well-known that large values of these magnitudes make the control system sensitive to process variations [2].

Each of the two constraints imply that the Nyquist curve of the loop-transfer function G avoids one circular disc in the complex plane. Consequently, the constraints are not convex in the optimization variable θ. However, the comparison with results of [21] in Section 5.4 indicates that minimization of the IAE constrained by $\|S\|_\infty \leq M_s$ and $\|T\|_\infty \leq M_t$ lacks local minima for industrially relevant plant models P and constraint levels M_s, M_t.

2.2.3. Noise Attenuation: The probably most common way to quantify activity of the control signal u, is through the variance σ_u^2, as in for example LQG control. In this work, a constraint on the standard deviation ratio σ_u/σ_n (or equivalently the variance ratio σ_u^2/σ_n^2) is considered. This is closely related to limiting the noise gain, defined in [6] as the ratio σ_u/σ_{y_f} between the standard deviations of the control signal and filtered measurement signal $y_f(s) = F(s)y(s)$. However, our definition has the advantage of being independent of the filter dynamics.

If an estimate $\hat{\sigma}_n$ of σ_n is available (it can be obtained in open-loop at the input of F), one can constrain an upper bound $\bar{\sigma}_u$ on σ_u through $M_q = \bar{\sigma}_u/\hat{\sigma}_n$.

In Section 4.2 we will see how two different assumptions on the spectral density of n lead to $\mathcal{H}_2$ and $\mathcal{H}_\infty$ constraints on Q, respectively.

3. Optimization

3.1. Gradient Methods

It was pointed out in [18] that the efficiency of solving (8) (without considering the constraint on Q) can be significantly improved by moving from gradient-free methods to gradient-based ones. Such methods rely on (approximations) of the objective and constraint gradients, with respect to the optimization variable. It is well-known that the convergence rate of gradient methods is significantly improved if exact gradients are supplied, as opposed to finite difference approximations. Furthermore, exact gradients improve accuracy for cases where the cost is flat in a vicinity of the

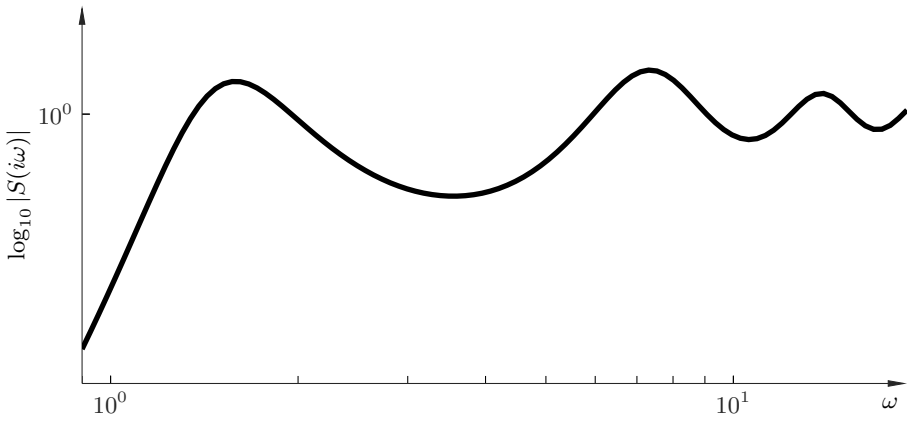

Fig. 2. *Sensitivity magnitude with multiple peaks, obtained during gradient search for IAE optimal controller. The example was obtained with* $P(s) = e^{-s}/(s+1)$, $C(s) = 1 + 4/s$, *and* $F(s) = 1$.

optimum.

Implementation of an active-set-based method for constrained optimization of PID parameters was presented in [11], see Section 1.2. While not relying on exact gradients, the method performs adequately on several test cases, but encounters difficulties with some dynamics, including $P(s) = e^{-s}/(s+1)$, and $P(s) = 1/(s+1)^4$.

Next, we will introduce two measures to improve convergence of gradient methods: the discretization of $\mathcal{H}_\infty$ constraints in Section 3.2 and the use of exact gradients in Section 3.3.

3.2. Constraint Discretization

The $\mathcal{H}_\infty$ constraint on S often poses a problem for gradient-based methods, as pointed out in [18]. The reason is that close to the optimal solution, it is common for the sensitivity function to have several sensitivity peaks of equal magnitude. This results in the optimizer discretely jumping between these peaks in subsequent iterations. The situation is illustrated in Figure 2. One solution to this problem, as proposed in [18], is to discretize the $\mathcal{H}_\infty$ constraint on S over a frequency grid $\Omega = \{\omega_1 < \omega_2 < \ldots, \omega_m\}$, resulting in m (number of grid points) constraints

$$|S(i\omega_k)| \leq M_s, k = 1, \ldots, m. \tag{9}$$

Instead of requiring $\|S\|_\infty \leq M_s$, it is required that $|S(i\omega)| \leq M_s, \forall \omega \in \Omega$. This modification is adopted for *all* $\mathcal{H}_\infty$ constraints in this paper.

For the examples in this paper, a grid based on P is *a priorily* chosen, consisting of $m = 500$ logarithmically spaced grid points between the -5° and -355° phase angles of P. This choice was motivated by extensive verification, see Section 5.4.

An alternative would be to produce the grid iteratively, using for instance the cutting set method suggested in [22]. It could also be mentioned that the KYP lemma provides an alternative formulation, altogether avoiding frequency gridding [23]. However, this formulation brakes down for (continuous) time processes with time delay, which is why it has not been applied in this paper.

3.3. Exact Gradients

3.3.1. Objective Gradient: The exact gradient of the objective, with respect to the optimization variable can be expressed

$$\nabla \text{IAE} = \int_0^\infty \text{sign}\left(e(t)\right) \nabla e(t) dt. \tag{10}$$

It was shown in [18] that the integral (10) can be evaluated by utilizing the fact that $\nabla e(t) = \mathcal{L}^{-1}(\nabla e(s))$. From the definition (5) of e, it is clear that $\nabla e(t) = \mathcal{L}^{-1}(P(s)\nabla S(s)/s)$, and we have

$$\nabla S = -S^2 \nabla G, \tag{11}$$

$$\nabla G = \nabla PCF = P(\nabla C)F + PC\nabla F, \tag{12}$$

$$\nabla C = \begin{bmatrix} 1 & 1 & 1 & 0 \end{bmatrix}, \tag{13}$$

$$\nabla F = \begin{bmatrix} 0 & 0 & 0 & \partial F/\partial T_f \end{bmatrix}, \tag{14}$$

$$\partial F/\partial T_f = -F^2 T_f \left(2s + T_f/\sqrt{2}\right). \tag{15}$$

This allows us to evaluate $\nabla e(t)$ through a step response simulation of ∇S, defined through (11)–(15), which in term enables the evaluation of (10).

If, instead, the IE is used, the minimization objective becomes $-k_i$ (see Section 2.2.1), with corresponding gradient $\nabla(-k_i) = \begin{bmatrix} 0 & -1 & 0 & 0 \end{bmatrix}$.

3.3.2. Robustness Constraint Gradients: The gradients of the discretized robustness constraints $\nabla|S|$ and $\nabla|T|$, see Section 3.2, were presented in [18]. In this paper, we will utilize the fact that the constraints represent circular discs, which must be avoided by the open-loop transfer function G. Expressions for the centra c_c and radii r_c of these constraint discs, as functions of the constraint levels M_s and M_t, are found in [2]. This allows for an equivalent reformulation of the robustness constraints on the form

$$|G - c_c| - r_c \leq 0, \tag{16}$$

where $|S| \leq M_s$ and $|T| \leq M_t$ corresponds to

$$c_s = -1, \qquad r_s = \frac{1}{M_s}, \qquad c_t = -\frac{M_t^2}{M_t^2 - 1}, \qquad r_t = \frac{M_t}{M_t^2 - 1}. \tag{17}$$

The advantage of this reformulation is that it yields less complicated expressions for both the constraints (16) and their gradients

$$\nabla|G - c_c| - r_c = \frac{1}{|G - c_c|}\text{Re}\left(G^* \nabla G\right), \tag{18}$$

where * denotes conjugation: $G^*(s) = -G(-s)$, and ∇G can be evaluated using (12)–(15).

4. Noise Attenuation

4.1. Filter structure

A second order measurement filter, (2), is chosen to guarantee high frequency roll-off. The filter has a fixed damping ratio as suggested in [3]. (Note that the damping ratio ζ is that of the filter poles, whereas ζ is used in [11] to denote the damping ratio of the filtered controller zeros.) It is possible to treat $\zeta > 0$ as a free optimization parameter, but experience has shown that this will only marginally increase performance, while significantly increasing computation time.

4.2. Variance Bounds

This section is devoted to the last constraint of (8), namely that on the noise amplification ratio σ_u/σ_n. The purpose of the constraint is to limit variance of the control signal u, resulting from the noise n, not to exceed a user-specified tolerable level σ_u^2. The variance σ_n^2 is assumed to be known (it can easily be estimated in open-loop). For cases where σ_n^2 is not known, the constraint level M_q of (8) can be considered a free tuning parameter, constituting a trade-off between performance (IAE) and noise attenuation (σ_u/σ_n).

Two cases will be studied: one for (band-limited) white noise in Section 4.2.1, and one for noise of unknown spectral density in Section 4.2.2.

4.2.1. White Noise: White noise n is characterized by a constant spectral density $\Phi_n(\omega) = \Phi_0$, resulting in infinite variance, or equivalently, infinite energy. However, white noise does not occur in nature, where the bandwidth of any signal is limited by the mechanism by which it is generated or measured. We will denote by ω_B the bandwidth of the sensor used in the control system. (For a periodically sampled digital controller, the Nyquist frequency constitutes an upper bound on ω_B.) The variance of the noise seen by the sensor is

$$\sigma_n^2 = \frac{1}{2\pi}\int_{-\omega_B}^{\omega_B} \Phi_0 d\omega = \frac{\omega_B}{\pi}\Phi_0, . \tag{19}$$

The resulting control signal variance is

$$\sigma_u^2 = \frac{1}{2\pi}\int_{-\omega_B}^{\omega_B} \Phi_0 |Q(i\omega)|^2 d\omega = \sigma_n^2 \|Q\|_2^2, \tag{20}$$

where the last equality holds as a consequence of the aforementioned band-limiting sensor. If the noise is (assumed to be) white, we consequently choose the $\mathcal{H}_2$ constraint

$$\frac{1}{\pi}\int_0^{\infty} |Q(i\omega)|^2 d\omega = \|Q\|_2^2 \leq M_q^2, \tag{21}$$

with corresponding gradient

$$\nabla \frac{1}{\pi}\int_0^{\infty} |Q(i\omega)|^2 d\omega = \frac{2}{\pi}\int_0^{\infty} |Q(i\omega)| \nabla |Q(i\omega)| d\omega, \tag{22}$$

where

$$\nabla |Q| = \frac{|S|}{|CF|}\left(|C|^2 \mathrm{Re}(SF^*\nabla F) + |F|^2 \mathrm{Re}(SC^*\nabla C)\right). \tag{23}$$

4.2.2. Unclassified Noise: If the spectral density of n is unknown, we will instead make use of the following inequality

$$\sigma_u^2 = \frac{1}{2\pi}\int_{-\infty}^{\infty} |Q(i\omega)|^2 \Phi_n(\omega) d\omega \leq \|Q\|_\infty^2 \frac{1}{2\pi}\int_{-\infty}^{\infty} \Phi_n(\omega) d\omega = \|Q\|_\infty^2 \sigma_n^2, \tag{24}$$

which can be rewritten $\sigma_u/\sigma_n \leq \|Q\|_\infty$. Consequently, constraining the $\mathcal{H}_\infty$ norm of Q by M_q (conservatively) guarantees $\sigma_u/\sigma_n \leq M_q$, regardless of the spectral density of n. Upon discretization, motivated in Section 3.2, this corresponds to a set of constraints (one for each frequency $\omega \in \Omega$) on the form

$$|Q| = \frac{|CF|}{|1+G|} \leq M_q, \tag{25}$$

$$|CF| - M_q|1+G| \leq 0. \tag{26}$$

The corresponding gradients are given by

$$\nabla|CF| - M_q \nabla|1+G|, \tag{27}$$

and can be evaluated using the methodology of Section 3.3.

4.3. Filter Time Constant Bounds

In order to avoid solutions where the filter time constant T_f is unbound from above, it is essential to achieve high-frequency roll-off within the frequency grid Ω. This is done by constraining the corner frequency $\omega_f = 1/T_f$ of F to lie below the highest frequency ω_m of the grid. Similarity, ω_f needs to lie above the smallest grid frequency ω_1 in order to avoid solutions which are unbound from below. Consequently, the following hard constraints are imposes:

$$\omega_1 \leq \omega_f \leq \omega_m. \tag{28}$$

The corner frequency ω_d, introduced by derivative action, is

$$\omega_d = -\arg\min_{|s|} |C(s) = 0| = \frac{1}{2k_d}|s_0|, \tag{29}$$

$$s_0 = k_p + \sqrt{k_p^2 - 4k_i k_d}. \tag{30}$$

Derivative action is lost if $\omega_d > \omega_f$, as illustrated in Figure 3. This may cause ambiguity in the solution of (8). It can be avoided by enforcing $\omega_d \leq \omega_f$ through the equivalent constraint

$$T_f|s_0| - 2k_d \leq 0, \tag{31}$$

with corresponding gradient

$$\nabla\left(T_f|s_0| - 2k_d\right) = \frac{T_f}{|s_0|}\mathrm{Re}\left(s_0^* \nabla s_0\right) + \begin{bmatrix} 0 & 0 & -2 & |s_0| \end{bmatrix}, \tag{32}$$

$$\nabla s_0 = \frac{1}{s_0 - k_p}\begin{bmatrix} s_0 & -2k_d & -2k_i & 0 \end{bmatrix}. \tag{33}$$

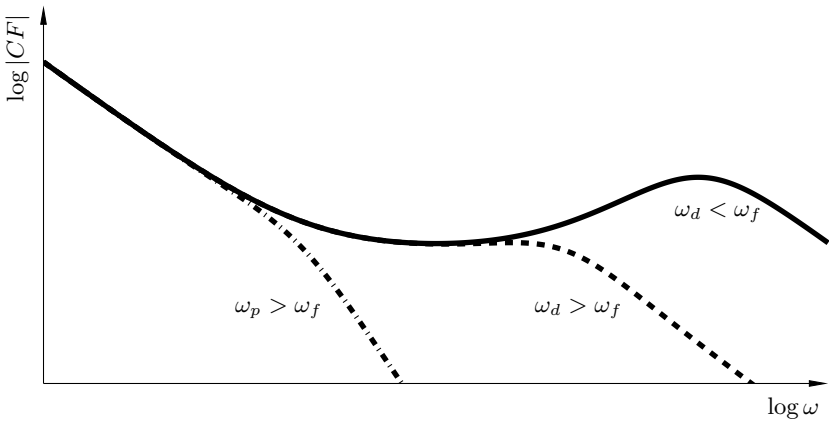

Fig. 3. *Bode magnitude of PID controller with combined measurement filter (solid) and the same controller with two slower filters resulting in the loss of derivative action (dashed) and proportional action (dashed-dotted).*

For controllers with $k_d = 0$, integral action is lost if $\omega_p > \omega_f$, where $\omega_p = k_i/k_p$ is the corner frequency corresponding to the zero introduced by proportional action. However, this situation never arises if (31) is imposed. For $k_d = 0$, (31) then becomes $2k_pT_f \leq 0$, which can only be fulfilled with $k_p = 0$ due to (28). Either the optimization will produce a controller with $k_d > 0$, for which case (31) is valid, or an I (purely integrating) controller, for which (28) provides sufficient bounds on T_f, since the I controller lacks zeros.

It should be noted that the above does not exclude any PID controller subtypes. For instance, filtered PI behavior is achieved at the limit $\omega_d \to \omega_f$. More importantly, the user does not have to make an *a priori* PID subtype selection (such as to include or exclude derivative action), as this is handled implicitly by the optimization.

5. Results

5.1. Method Summary

Before considering a case example in Section 5.2, the method outlined in Section 2 through Section 4, is briefly summarized below.

1. Obtain a model P of the plant to be controlled (using any method).
2. Impose robustness constraint levels M_s and (possibly) M_t.
3. Decide on an upper bound on the control signal variance $\bar{\sigma}_u^2$, induced by measurement noise. Obtain a measurement or estimate $\hat{\sigma}_n^2$ of the noise variance, and set the constraint level $M_q = \bar{\sigma}_u/\hat{\sigma}_n$. If n can be assumed to be white, impose an $\mathcal{H}_2$ constraint on the noise sensitivity Q, otherwise an $\mathcal{H}_\infty$ constraint.
4. Construct a frequency grid Ω, and discretize all $\mathcal{H}_\infty$ constraints according to Section 3.2.
5. Solve (8) using a gradient method, and provide it with exact gradients, as defined throughout the paper.

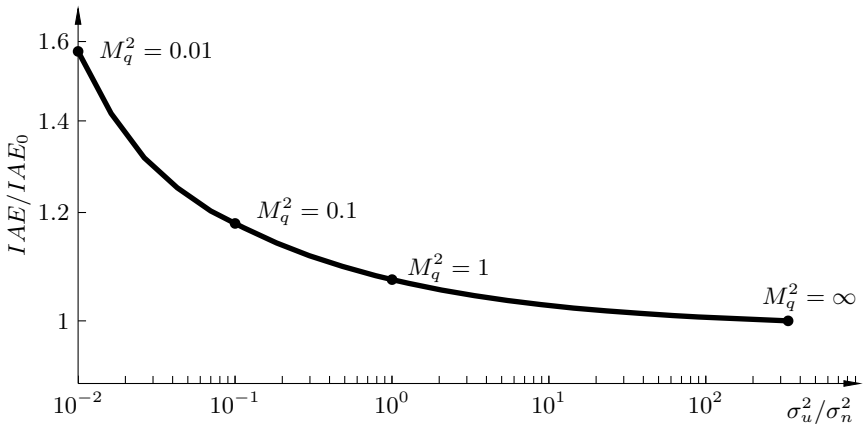

Fig. 4. *Pareto front, relating σ_u^2/σ_n^2, constrained by M_q^2, to performance decrease IAE/IAE_0. The objective IAE_0 results from the unconstrained case $M_q = \infty$. Markers correspond to the controllers evaluated in Figure 6.*

5.2. Case Example

The proposed synthesis method is demonstrated through a realistic example, in which the plant to be controlled is

$$P(s) = \frac{e^{-s}}{s+1}. \tag{34}$$

This structure is a commonly used model in process industry, where higher-order dynamics are often lumped together and distributed between the time constant and delay. It should, however, be noted that the method proposed herein can be used directly on higher-order dynamical models, when such are available – see Section 5.3 for an example.

In order to demonstrate the effects of the noise constraint, the system is subject to white noise of standard deviation $\sigma_n = 0.1$, band-limited by the Nyquist frequency corresponding to the controller sampling period $h = 0.02$ (chosen to give 100 samples per average residence time of P). Robustness constraints are fixed at industrially relevant values of $M_s = M_t = 1.4$, and it is (correctly) assumed that the noise is white, i.e., the case of Section 4.2.1 is considered.

The optimization problem (8) and corresponding constraint gradients were provided to a solver (invoked through the Matlab `fmincon` command). The solution for unconstrained noise sensitivity ($M_q = \infty$) is shown on the last row of Table 1. The large corresponding value $\|Q\|_2 \approx 125$ results in high noise amplification from n to u, as shown in the light grey curve of Figure 5.2. For most industrial scenarios, this would result in unacceptable, actuator wear.

By solving (8) for additional values of M_q, we obtain the Pareto front shown in Figure 4. It relates the (variance ratio) constraint level M_q^2 to the corresponding increase in optimization objective. The controller and filter parameters corresponding to the design cases shown in Figure 4 are enlisted in Table 1. Bode plots for CF of Table 1 are shown in Figure 5. They clearly show how smaller values of M_q result in more aggressive filtering, at the cost of losing phase advance.

In order to illustrate the trade-off, controllers corresponding to the (variance ratio) constraint levels $M_q^2 \in \{0.01, 0.1, 1, \infty\}$, marked in Figure 4, were evaluated in a load unit step test. The resulting plant outputs y and control signals u are shown in Figure 6.

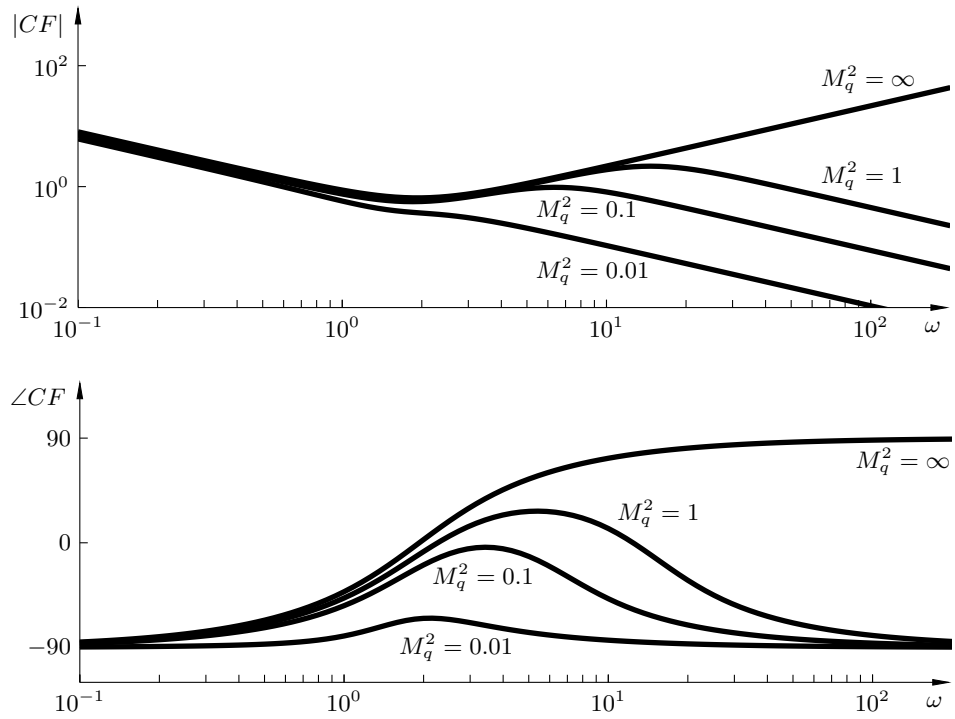

Fig. 5. *Bode plots of Pareto-optimal controller with filter, CF, from Table 1.*

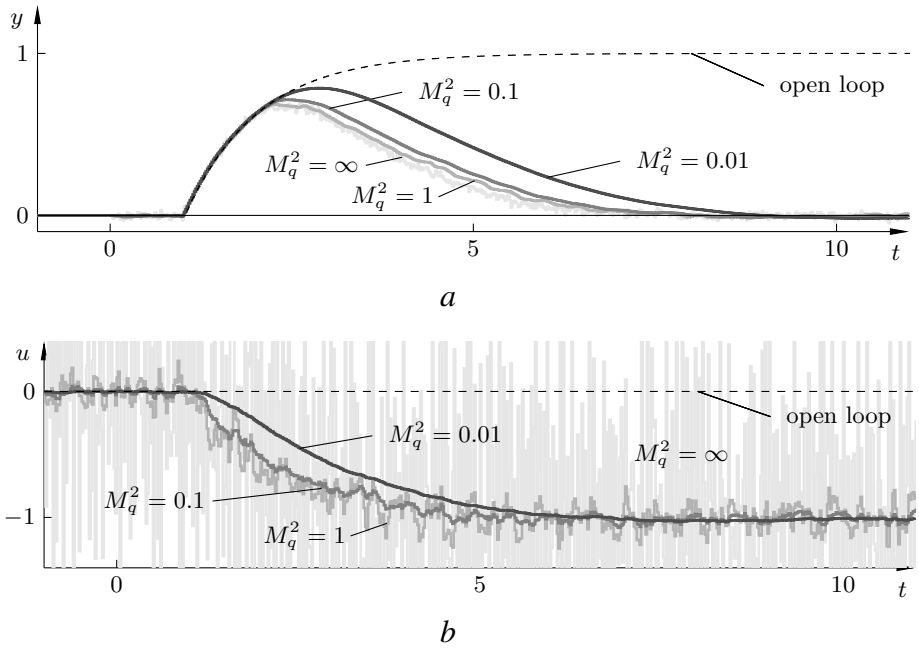

Fig. 6. *Simulated response to load step disturbances for four Pareto optimal controllers, obtained with $M_q^2 = 0.01$ (black), $M_q^2 = 0.1$ (dark grey), $M_q^2 = 1$ (grey) and $M_q^2 = \infty$ (light grey, truncated). Dashed line shows open-loop disturbance response (with $u = 0$).*
a Plant output y
b Control signal u

Table 1 Parallel form (4) PID parameters and filter time constant T_f, together with increase in IAE compared with IAE_0, resulting from $M_q = \infty$.

M_q^2	K	T_i	T_d	T_f	IAE/IAE_0
0.01	0.461	0.748	0.530	0.478	1.57
0.1	0.566	0.796	0.374	0.155	1.18
1	0.612	0.806	0.341	0.068	1.07
∞	0.651	0.809	0.333	$1/\omega_m \approx 0$	1.00

5.3. Case Example 2

In order to demonstrate the usefulness of the method on more complicated dynamics, a process with two poles, one zero and time delay is considered:

$$P(s) = \frac{s+2}{(s+1)(s+5)}e^{-3s}. \tag{35}$$

We will again consider $\sigma_n^2 = 0.1$. For this example, the noise constraint is fixed to $M_q = 1$, while different levels or robustness, constituted through $M = M_s = M_t \in \{1.2, 1.4, 1.6\}$, are evaluated. The load disturbance responses of resulting control systems are shown in Figure 7. In this particular case, there is no major performance loss associated with an increase in robustness margin from $M = 1.6$ to $M = 1.2$.

5.4. Verification

For the very simple case of unconstrained PI control of $P(s) = e^{-sL}/s$ (delayed integrator), the problem (8) has been shown to be convex [24]. The likely lack of convexity for other instances of (8) is, however, not sufficient for the existence of local minima. Furthermore, it is possible to construct cases which do hold local minima. One example is conditionally stable plants, as described in [25]. To the knowledge of the authors there exists no complete classification of which cases result in local minima.

In order to verify optimality of solutions provided by the proposed method, it was evaluated over a set industrially representative process dynamics. This set constitutes the AMIGO test batch, found in [2]. Optimal PID and filter parameter for several constraint levels for the set were recently reported in [21]. The proposed method found the optimal solution (within numerical tolerance imposed by Ω) for all test cases. Execution times ranged 2–10 s on a standard desktop computer. (The code was not optimized for speed.) In all cases, including the examples of Section 5.2 and Section 5.3, the method was initialized with the IE-optimal PID controller with fixed $F = 1$, found using the convex-convave procedure presented in [26].

6. Conclusion

A method for simultaneous PID controller and measurement filter design has been proposed. The method minimizes the load step IAE, under constraints enforcing robustness and noise attenuation.

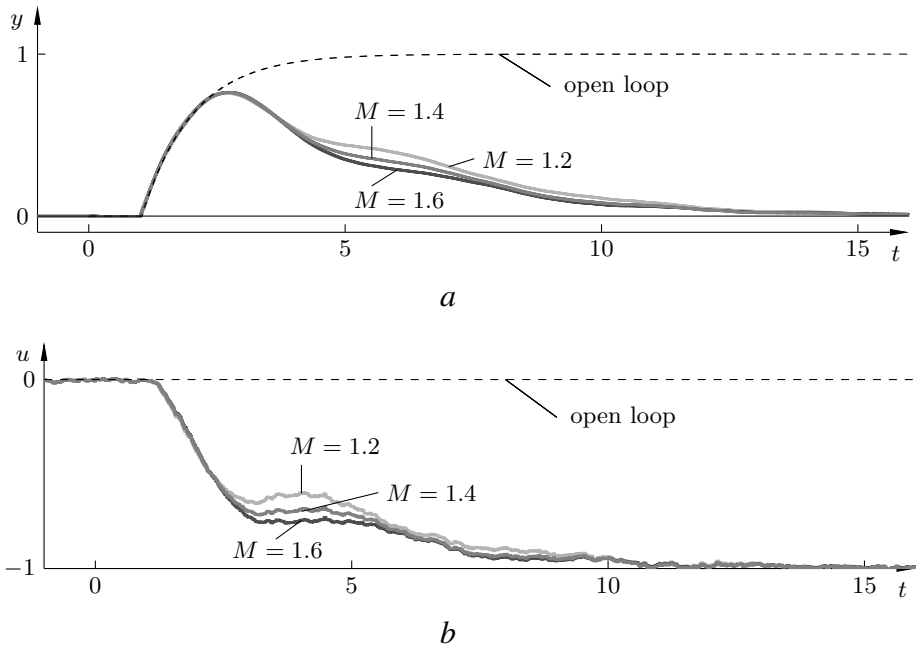

Fig. 7. *Simulated response to load step disturbances. Three controllers were synthesized for the plant (35), with $M_q^2 = 1$ and $M = 1.2$ (light grey), $M = 1.4$ (grey), $M = 1.6$ (dark grey).*
a Plant output y
b Control signal u

The corresponding constraint level can be viewed as a free design parameter, constituting a trade-off between performance and noise attenuation from the control signal. Typically, as illustrated by Figure 6, an increase in noise attenuation performance comes at the cost of decreased load attenuation performance.

The main novelty lies in the use of explicit gradient of the objective and constraint functions with respect to the optimization variable. This makes the proposed method more robust than if finite difference approximations would be utilized.

Selection of PID subtype (such as PI, P, or PID) is handled implicitly by the optimization - no *a priori* selection is necessary.

Numeric robustness and optimality of the proposed method has been demonstrated through evaluation over a large set of industrially relevant design scenarios, for which the optimal solutions have been previously reported.

Acknowledgements

We would like to acknowledge Olof Garpinger, for valuable input on references to prior work. This work was partially financed by Kungliga Ingenjörsvetenskapsakademien (IVA), and by the Vinnova strategic program PiiA. The first author would also like to acknowledge the Lund University LCCC and ELLIIT research centra.

References

[1] Hast, M. and Hägglund, T.: 'Optimal proportional–integral–derivative set-point weighting and tuning rules for proportional set-point weights', IET Control Theory & Applications, 2015, **9**, (15)

[2] Åström, K. J. and Hägglund, T.: 'Advanced PID Control' (ISA - The Instrumentation, Systems, and Automation Society, 2006, 1st edn.)

[3] Larsson, P.-O. and Hägglund, T.: 'Comparison Between Robust PID and Predictive PI Controllers with Constrained Control Signal Noise Sensitivity'. Proc. Conference on Advances in PID Control, Brescia, Italy: IFAC, 2012

[4] Šekara, T. B. and Mataušek, M. R.: 'Optimization of PID Controller Based on Maximization of the Proportional Gain Under Constraints on Robustness and Sensitivity to Measurement Noise', IEEE Transactions on Automatic Control, 2009, **54**, (1), pp. 184–189

[5] Panagopoulos, H., Åström, K. J., and Hägglund, T.: 'Design of PID controllers based on constrained optimisation', Control Theory and Applications, IEEE proceedings of, 2002, **149**, (1), pp. 32–40

[6] Romero Segovia, V., Hägglund, T., and Åström, K. J.: 'Measurement noise filtering for PID controllers', Journal of Process Control, 2014, **24**, (4), pp. 299–313

[7] Garpinger, O. and Hägglund, T.: 'Software-based optimal PIDdesign with robustness and noise sensitivity constraints', Journal of Process Control, 2015, **33**, pp. 90–101

[8] Kristiansson, B. and Lennartson, B.: 'Robust and optimal tuning of PI and PID controllers', Control Theory and Application, IEEE proceedings of, 2002, **149**, (1), pp. 17–25

[9] Kristiansson, B. and Lennartson, B.: 'Evaluation of simple tuning of PID controllers with high-frequency robustness', Journal of Process Control, 2006, **16**, (2), pp. 91–102

[10] Balchen, J. G.: 'A performance Index for Feedback Control Systems Based on the Fourier Transform of the Control Deviation', Acta Polytechnica Scandinavica, 1958, **247**, pp. 1–18

[11] Lennartson, B.: 'Multi Criteria Hinf Optimal PID Controllers from an Undergraduate Perspective'. Proc. IFAC Conference on Advances in PID Control, Brescia, Italy, 2012

[12] Leva, A. and Maggio, M.: 'A systematic way to extend ideal PID tuning rules to the real structure', Journal of Process Control, 2011, **21**, (1), pp. 130–136

[13] Romero Segovia, V., Hägglund, T., and Åström, K. J.: 'Measurement noise filtering for common PID tuning rules', Control Engineering Practice, 2014, **32**, pp. 43–63

[14] Skogestad, S.: 'Simple analytic rules for model reduction and PID controller tuning', Journal of Process Control, 2003, **13**, (4), pp. 291–309

[15] Åström, K. J. and Hägglund, T.: 'Revisiting the Ziegler-Nichols step response method for PID control', Journal of Process Control, 2004, **14**, pp. 635–650

[16] Micić, A. D. and Mataušek, M. R.: 'Optimization of PID controller with higher-order noise filter', Journal of Process Control, 2014, **24**, (5), pp. 694–700

[17] Larsson, P.-O. and Hägglund, T.: 'Control Signal Constraints and Filter Order Selection for PID Controllers'. Proc. American Control Conference, Proceedings of, San Francisco, California, USA, 2011

[18] Grimholt, C. and Skogestad, S.: 'Improved Optimization-based Design of PID Controllers Using Exact Gradients'. Proc. European Symposium on Computer Aided Process Engineering, Copenhagen, Denmark, 2015

[19] Garpingar, O. and Hägglund, T.: 'A Software Tool for Robust PID Design'. Proc. 17th IFAC-World Congress, Seoul, Korea, 2008

[20] Åström, K. J., Panagopoulos, H., and Hägglund, T.: 'Design of PI controllers based on non-convex optimization', Automatica, 1998, **34**, (5), pp. 585–601

[21] Garpinger, O.: 'Optimal PI and PID Parameters for a Batch of Benchmark Process Models Representative for the Process Industry', Technical Report 7645, Dept. Automatic Control, Lund University, Sweden, 2015

[22] Lipp, T. and Boyd, S.: 'Variations and Extensions of the Convex-Concave Procedure', 2014

[23] Hara, S., Iwasaki, T., and Shiokata, D.: 'Robust PID control using generalized KYP synthesis: direct open-loop shaping in multiple frequency ranges', Control Systems, IEEE, 2006, **26**, (1), pp. 80–91

[24] Esch, J., Knings, T., and Ding, S. X.: 'Optimal Performance Tuning of a PI-Controller for an Integrator Plant with Uncertain Parameters as a Convex Optimisation Problem'. Proc. 52nd Conference on Decision and Control, IEEE, 2013, pp. 1977–1982

[25] Gerry, J. P.: 'Conditionally Stable Tuning of PI and PID Controllers on Common Processes'. Proc. American Control Conference, IEEE, 1984, pp. 512–517

[26] Hast, M., Åström, K. J., Bernhardsson, B., and Boyd, S. P.: 'PID Design by Convex-Concave Optimization'. Proc. 2013 European Control Conference, Zürich, Switzerland, 2013